Hindawi Publishing Corporation
Journal of Nanomaterials
Volume 2015, Article ID 970856, 7 pages
http://dx.doi.org/10.1155/2015/970856

Research Article

Morphology Effect on Enhanced Li^+-Ion Storage Performance for $Ni^{2+/3+}$ and/or $Co^{2+/3+}$ Doped $LiMnPO_4$ Cathode Nanoparticles

Young Jun Yun,[1,2] Mihye Wu,[1] Jin Kyu Kim,[1] Ji Young Ju,[1] Sun Sook Lee,[1] Ki Woong Kim,[1] Woon Ik Park,[3] Ha-Kyun Jung,[1] Kwang Ho Kim,[3,4] Jin-Seong Park,[2] and Sungho Choi[1]

[1]*Advanced Battery Materials Research Group, Korea Research Institute of Chemical Technology, 141 Gajeongro, Yuseong, Daejeon 305-600, Republic of Korea*
[2]*Division of Materials Science and Engineering, Hanyang University, Seongdong-gu, Seoul 133-791, Republic of Korea*
[3]*Global Frontier R&D Center for Hybrid Interface Materials (HIM), Busandaehak-ro 63 beon-gil, Geumjeong-gu, Busan 609-735, Republic of Korea*
[4]*School of Materials Science and Engineering, Pusan National University (PNU), Busandaehak-ro 63 beon-gil, Geumjeong-gu, Busan 609-735, Republic of Korea*

Correspondence should be addressed to Kwang Ho Kim; kwhokim@pusan.ac.kr, Jin-Seong Park; jsparklime@hanyang.ac.kr, and Sungho Choi; shochoi@krict.re.kr

Received 24 August 2015; Accepted 4 November 2015

Academic Editor: Je M. Yun

The electrochemical performance of $Li(Mn, M)PO_4$ ($M = Co^{2+/3+}, Ni^{2+/3+}$) was investigated with regard to the particle morphology. Within a controlled chemical composition, $Li(Mn_{0.92}Co_{0.04}Ni_{0.04})PO_4$, the resultant cathode exhibited somewhat spherical-shaped nanocrystalline particles and enhanced Li^+-ion storage, which was even better than the undoped $LiMnPO_4$, up to 16% in discharge capacity at 0.05 C. The outstanding electrochemical performance is attributed to the well-dispersed spherical-shaped particle morphology, which allows the fast Li^+-ion migration during the electrochemical lithiation/delithiation process, especially at high current density.

1. Introduction

Nowadays, demand for medium and large scale batteries has grown owing to the development of such applications as electric vehicles (EV), hybrid electric vehicles (HEV), and energy storage system (ESS) [1, 2]. Consequently, it is of great importance to develop new cathodes with greater energy and power densities for the next generation of Li ion batteries.

Although there are diverse cathode materials that meet the requirements of this demand, $LiMPO_4$ (M = Fe, Mn, Co, and Ni) olivine compounds are being seriously considered as cathode materials for Li ion batteries because of their great structural stability and electrochemical performance. Olivine compounds do not suffer from structural rearrangement by the lithiation and delithiation of Li^+-ions, based on the PO_4^{3-} tetrahedral polyanions; the strong covalent bonds between the oxygen and the P^{5+} ions stabilize the three-dimensional framework of the olivine structure [3]. Therefore, $LiMPO_4$ electrodes have substantially better stability and capacity retention along with continued cycling compared with other transition-metal oxide cathode materials such as $LiCoO_2$, $LiNiO_2$, $LiMnO_2$, and $LiMn_2O_4$ [4, 5]. Moreover, due to the excellent cycle life, high capacity, and thermal stability of olivine-type materials, these materials have been substantially investigated as promising electrode materials for rechargeable Li ion batteries [6–8]. Among the diverse olivine-type materials, $LiFePO_4$ has already been used as commercial cathode material in Li ion batteries. However, $LiFePO_4$ suffers from a critical problem: it has a relatively low operating voltage region (3.4 V versus Li/Li^+), which

results in limited energy density. Consequently, $LiMnPO_4$ as a representative of $LiMPO_4$ has attracted much attention for its high operating voltage region (4.1 V versus Li/Li^+), accompanied with high-energy density (697 Wh Kg^{-1}) [9, 10]. Despite this advantage, the inherent low electronic conductivity ($<10^{-10}$ S cm^{-1}) is one of the main causes that degrades the electrochemical performance of $LiMnPO_4$, which is manifested in poor cycle life and poor rate capability [11]. To overcome this limitation, many strategies have considered enhancing the electrochemical performance of $LiMnPO_4$: morphology control, particle size reduction, carbonaceous material coating, and cation substitution or doping [12–15].

It is generally known that downsizing electrode material to the nanoscale (50–100 nm) can remarkably improve Li^+-ion accessibility and enhance the electron transport. Moreover, nanosized electrode materials effectively buffer the large volume expansion/contraction and alleviate the strain caused during repeated Li^+-ion lithiation/delithiation, thereby improving the cycle life. In particular, cation doping has been proposed as one of the most effective and straightforward methods for improving the electrochemical properties of olivine-type electrode materials by improving the charge transfer ability [16]. Lee et al. also reported the enhancement of electrochemical performance of $LiMnPO_4$ by Mg doping without increasing the rate capability [17]. In addition, Kim et al. revealed that there are differences in Fe-Co codoped $LiMnPO_4$ and only Fe-doped $LiMnPO_4$ composition [18].

Here, we report the enhanced electrochemical performance of $LiMnPO_4$ according to the dopant ions and particle morphologies. Various cations were adopted in $LiMnPO_4$ via a microwave-assisted hydrothermal process, which has advantages such as simple and fast reaction process [19, 20]. The resultant $LiMnPO_4$ and cation-doped $LiMnPO_4$ exhibited nanorod and spherical morphologies, respectively, and we investigated their electrochemical performances along with the origins of their different properties. Different cations, such as Ni and Co, were applied into the $LiMnPO_4$ lattice. In particular, we prepared $LiMn_{0.9}Co_{0.1}PO_4$, $LiMn_{0.9}Ni_{0.1}PO_4$, and $LiMn_{0.92}Co_{0.04}Ni_{0.04}PO_4$ and investigated their performance as electrode materials in relation to charge-discharge curves, cycling stability, and rate capability.

2. Experiment

$Li(Mn_{1-x}M_x)PO_4$ (M = Ni, Co) was prepared by a microwave-assisted hydrothermal method. The raw materials were $Li(CH_3COO)\cdot 2H_2O$ (98%, Sigma Aldrich), $MnSO_4\cdot H_2O$ (99%, Sigma Aldrich), $CoSO_4\cdot 7H_2O$ (99%, Sigma Aldrich), $NiSO_4\cdot 7H_2O$ (99%, Sigma Aldrich), CTAB (cetyltrimethylammonium bromide), and H_3PO_4 (85%, High Purity Chemicals). The CTAB was used as a surfactant. In the synthesis of $Li(Mn_{1-x}M_x)PO_4$ (M = Ni, Co), the molar ratio of Li : (Mn, M) : P was 3 : 1 : 1, and then it was dissolved in 50 mL of 2-methoxy ethanol with vigorous stirring. Then, the cationic surfactant CTAB was dissolved in the above solution. The homogeneously dispersed solution was transferred to a 100 mL Teflon-liner and placed in a microwave irradiation system (Model MARS6, CEM Corp., USA). The solution was heated at 260°C and maintained for 1 hour. The as-obtained products were collected, washed several times with DI water, and dried at 90°C for 24 h. For the carbon-coating on the surface of the electrode particles, $LiMnPO_4$ powder was milled with 10 wt% of sucrose in ethanol by a planetary high-energy ball-milling (400 rpm, 3 h). After the ball-milling, the samples were put into an alumina boat in a furnace and annealed at 700°C for 1 h under reducing atmosphere (95% N_2/5% H_2).

The crystal structure of the products was investigated by powder X-ray diffraction (XRD) on a Rigaku Ultima IV Diffractometer using Cu K < radiation operating at 40 kV and 40 mA. The surface morphology of the synthesized particles was studied using a scanning electron microscope (FE-SEM, Tescan Mira 3 LMU FEG, 20 kV). X-ray photoelectron spectroscopy (XPS, K-Alpha Thermo Scientific) was used to characterize the chemical state of the elements.

The electrochemical performance was investigated using CR2032 coin type cells. The cathodes were prepared by blending the active materials $LiMnPO_4$, Super-P, and polyvinylidene fluoride (PVdF, Kureha KF-1100) as a binder in a weight ratio of 70 : 20 : 10 and then dissolved in NMP (*N*-methyl-2-pyrrolidone, Sigma Aldrich, 99.5%) solution. The mass loading of the active material was 1.2 mg/cm^2. The resulting slurry was spread on aluminum foil as a current collector (Doctor Blade method), pressed, and then vacuum-dried at 120°C for 12 h. Lithium metal was used as a negative electrode, and 1 M $LiPF_6$ dissolved in a mixture of ethylene carbonate diethyl carbonate (EC/DEC 1 : 1 v/v) was used as electrolyte. The assembly of the coin cells was carried out in a dry argon-filled glove box.

The galvanostatic charge-discharge capacity, rate capability, and cyclic performance were tested at current densities of C/20 (1 C = 170 mA g^{-1}) between 2.7 and 4.5 V versus Li/Li^+ using a multichannel battery testing equipment (TOSCAT-3100, Toyo Co.). Cyclic voltammetry (CV) was operated on a multi-electrochemical analyzer system (Bio-Logic VSP 0417) between 3.0 and 5.0 V at a scanning rate of 0.2 mV s^{-1}.

3. Results and Discussion

X-ray diffraction (XRD) patterns of $LiMnPO_4$, $LiMn_{0.9}Ni_{0.1}PO_4$, $LiMn_{0.9}Co_{0.1}PO_4$, and $LiMn_{0.92}Ni_{0.04}Co_{0.04}PO_4$ are shown in Figure 1(a). All the samples were single-phased with the ordered olivine structure of a Pnma orthorhombic system, which is in good agreement with the standard value (JCPDS 01-072-1237). After elemental substitution, there was no deviation in the peak position or the FWHM (Full With at Half Maximum), indicating that the elemental substitution results in no alteration of the crystalline structure.

To clarify the variations in the chemical state of Ni and Co elements, X-ray photoelectron spectroscopy (XPS) measurements were carried out, and the typical XPS spectra for Co 2*p* and Ni 2*p* for the $LiMn_{0.92}Ni_{0.04}Co_{0.04}PO_4$ are shown in Figure 1(b). As shown, the binding energies were observed at 780, 796, 854, and 872 eV, which are attributed to Co $2p_{3/2}$, Co $2p_{1/2}$, Ni $2p_{3/2}$, and Ni $2p_{1/2}$, assigned well

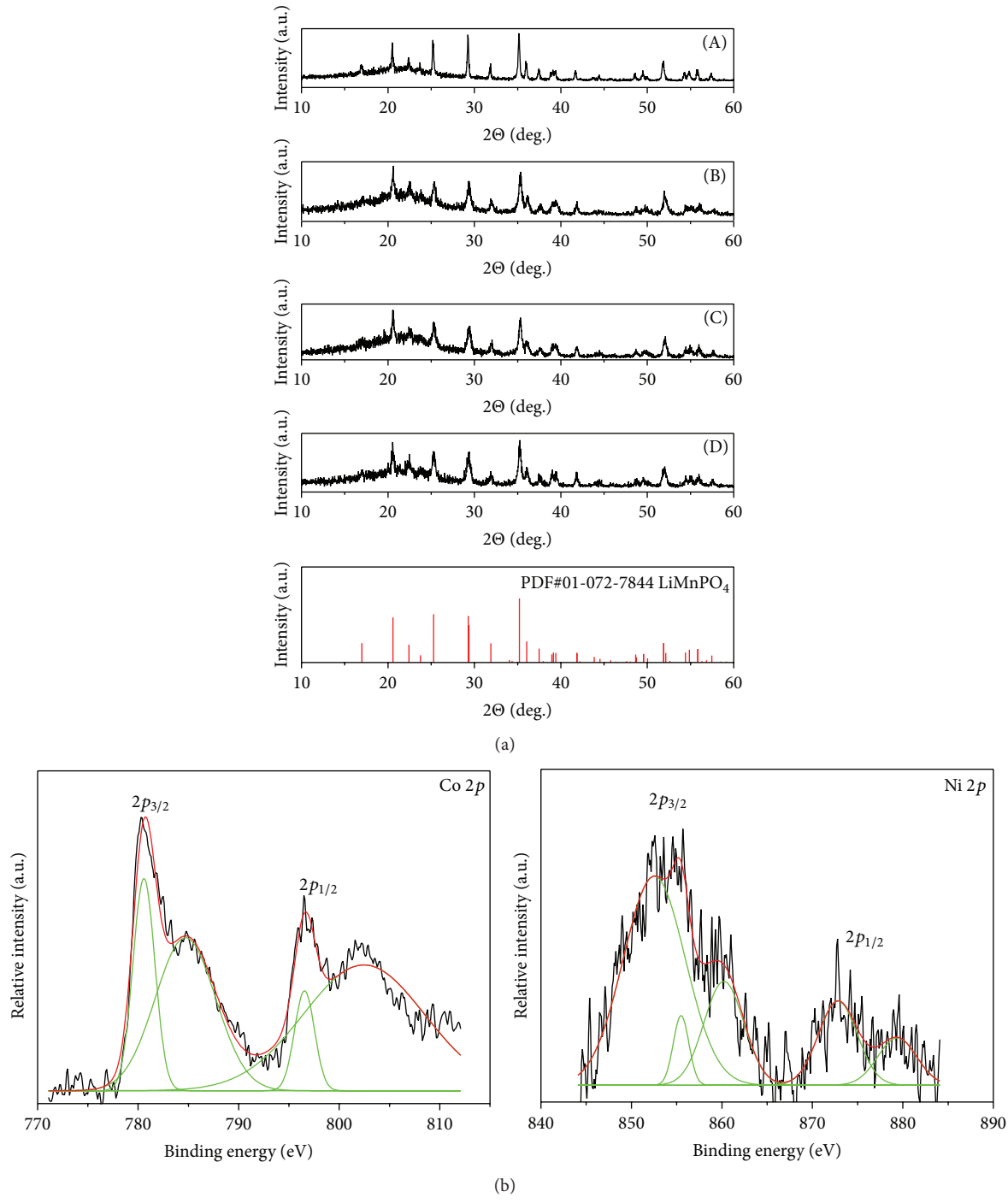

FIGURE 1: (a) The XRD spectra of (A) pristine, (B) Ni-doped, (C) Co-doped, and (D) Co-/Ni-doped $LiMnPO_4$ powders. (b) Co 2*p* and Ni 2*p* XPS spectra of Co-/Ni-doped $LiMnPO_4$.

with those for Co^{3+}/Co^{2+} and Ni^{3+}/Ni^{2+}, respectively [21, 22]. Regarding the chemical state of Ni and Co, we concluded that Co and Ni were successively doped on $LiMnPO_4$, which may provide notable electrochemical activities of the $LiMnPO_4$ as electrode materials.

The scanning electron micrographs (SEM) of as-obtained $LiMnPO_4$, $LiMn_{0.9}Ni_{0.1}PO_4$, $LiMn_{0.9}Co_{0.1}PO_4$, and $LiMn_{0.92}Ni_{0.04}Co_{0.04}PO_4$ samples are presented in Figure 2. As can be seen, the pristine $LiMnPO_4$ sample has a nanorod morphology with a diameter of about 40 nm, whereas all the Co-/Ni-doped $LiMnPO_4$ samples have spherical morphologies with a diameter of about 30 nm. Since the particle properties such as morphology and size have a great effect on the performance of Li ion batteries, $LiMnPO_4$ and Co-/Ni-doped $LiMnPO_4$ may exhibit different electrochemical features. When the particles were

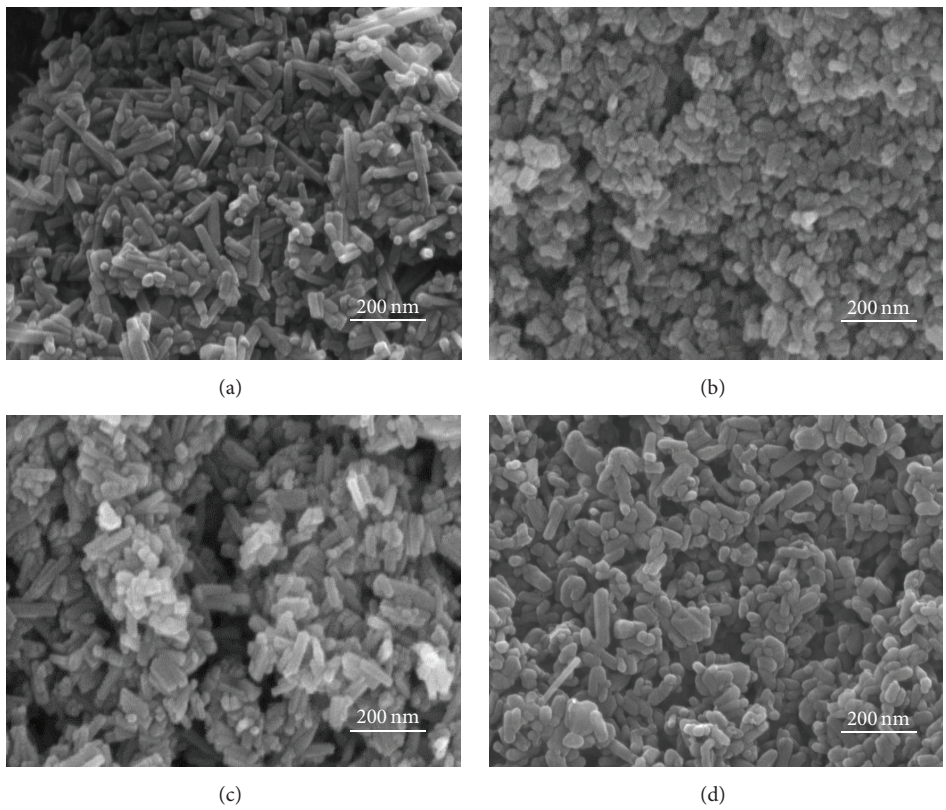

Figure 2: SEM images of (a) pristine, (b) Ni-doped, (c) Co-doped, and (d) Co-/Ni-doped $LiMnPO_4$ powders.

scaled down to nanoscale, the surface-to-volume ratios increased, leading to the high accessibility of Li^+-ions to the electrode materials during the lithiation/delithiation process. To obtain $LiMnPO_4$ with fine nanosized particles with excellent electrochemical properties, it is essential to use a hydrothermal method and add a surfactant because the electrochemical performance of the electrode is strongly related to the particle size, which determines the diffusion length and surface area for the reaction. By adopting CTAB as a surfactant, the grain size increase can be prevented, which demonstrates that CTAB can act as an internal reducing agent for homogenizing particle size [23, 24]. Not only does the intrinsically low electronic conductivity of $LiMnPO_4$ diminish the cathode performance, but also the anisotropic diffusion channels for Li^+-ions in the olivine structure result in low ionic conductivity. For this reason, controlling particle size and morphology is essential in preparing high performance $LiMnPO_4$ [15].

The cyclic voltammetry (CV) curves of $LiMnPO_4$ results presented in Figure 3 confirm the electrochemical reaction at the given voltage region. The reduction and oxidation peak of $LiMnPO_4$ are located at 3.85 and 4.35 V, respectively, indicating that the peak potential difference (ΔE_p) is about 0.5 V at a scan rate of 0.2 mV s^{-1}. These results confirm that the suitable oxidation/reduction reactions of the Mn^{2+}/Mn^{3+} redox couple exist in the olivine structure [3, 18, 25].

The voltage profiles of the $LiMnPO_4$ and Co-/Ni-doped $LiMnPO_4$ at different current densities are given in Figure 4.

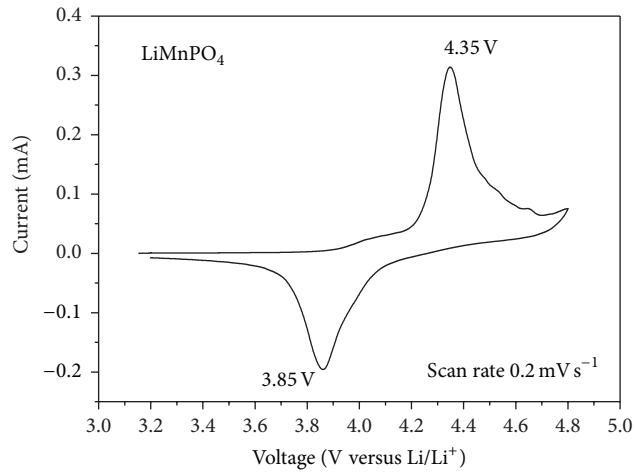

Figure 3: Cyclic voltammogram profile of $LiMnPO_4$ at 0.2 mV s^{-1} scan rate.

The initial charge-discharge curves of all the samples were tested at C/20 (8.5 mA g^{-1}) and are shown in Figure 4(a). The specific capacity of $LiMnPO_4$ was 115 mA h g^{-1}, which is 68% of the theoretical capacity. The problem of the olivine structure of $LiMnPO_4$ is its low electronic and ionic conductivity, so electrochemical properties are highly dependent on the kinetics of $LiMnPO_4$. The electrochemical properties of pure $LiMnPO_4$ are poor due to the blockage of the

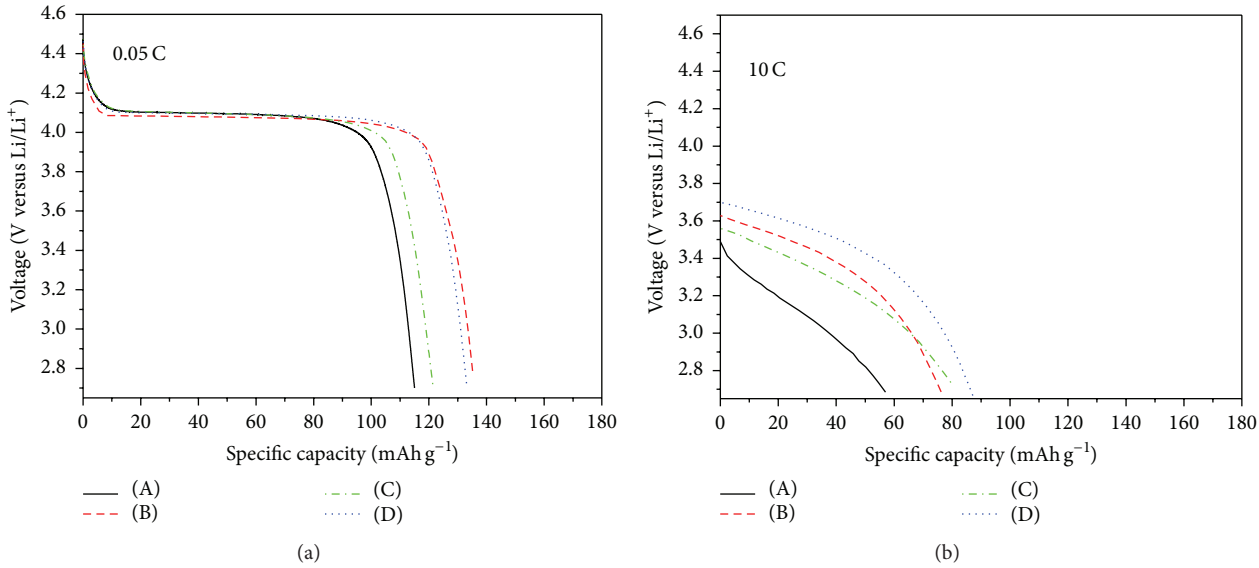

FIGURE 4: Initial discharge curves of (A) pristine, (B) Ni-doped, (C) Co-doped, and (D) Co-/Ni-doped $LiMnPO_4$ at current density of (a) C/20 and (b) 10 C.

diffusion path of the Li^+-ions by excess Mn^{2+} ions on Li sites, which deteriorates the capacity [26]. Furthermore, the electron transport is restricted by the strong Mn–O bonds, and the Li^+-ions diffusion is limited by the Li–O bonds. Thus, to improve the electrochemical properties of the samples obtained using the elemental substitution, we selected the transition metals Ni and Co. The initial discharge capacity of $LiMnPO_4$, $LiMn_{0.9}Ni_{0.1}PO_4$, $LiMn_{0.9}Co_{0.1}PO_4$, and $LiMn_{0.92}Ni_{0.04}Co_{0.04}PO_4$ was 115, 136, 121, and 134 mA h g^{-1}, respectively. At 10 C (1700 mA g^{-1}), the discharge capacity was 57 mA h g^{-1} for $LiMnPO_4$ (49% of the capacity at C/20), whereas the discharge capacity of $LiMn_{0.92}Ni_{0.04}Co_{0.04}PO_4$ was 88 mA h g^{-1} (66% at C/20). Clearly, the Co-/Ni-doped $LiMnPO_4$ achieved a higher capacity than pristine $LiMnPO_4$. The reason for the increment in the electrochemical properties of $LiMnPO_4$ is that the substitution of a small amount of Co and Ni in $LiMnPO_4$ led to a reduction in volume changes during the delithiation of Li^+-ions. Furthermore, the small binding energy of Li–O bonds makes it easy to migrate Li^+-ions [6, 27, 28]. Moreover, the pristine $LiMnPO_4$ exhibited a nanorod morphology, which has one-dimensional ionic diffusion paths, and the Co-/Ni-doped $LiMnPO_4$ showed a deviation in diffusion paths due to its spherical morphologies. Chen et al. experimentally demonstrated the movement of Li^+-ions in the olivine structure by studying the phase boundary through TEM [29]. The Li^+-ions migrated along the *b* direction, and it was also reported by Morgan et al. (or coworkers) that the $LiMPO_4$ with a nanorod morphology had a one-dimensional diffusion path along the [010] direction based on the space group of Pnma [30, 31]. As mentioned above, since one of the major constraints on the conductivity of Li^+-ions is that the diffusion channel of Li^+-ions is one-dimensional, we can infer that the diffusion of Li^+-ions may be alleviated by extending the diffusion paths. In particular, the lattice enlargement along the *a* direction facilitates the expansion of Li^+ diffusion channels, which sufficiently increases the mobility of Li^+-ions. Therefore, we assumed that the lattice parameter in the *a* direction was somewhat increased by the changing particle morphology from nanorod to spherical, which resulted in mitigating the diffusion of Li^+-ions in the $LiMnPO_4$ lattice. Thus, it is noteworthy that the diffusion of Li^+-ions can be improved not only by reducing the particle size to nanoscale but also by controlling the particle morphology.

To address the question of whether Co and Ni doping result in the improved electrochemical performance of $LiMnPO_4$, we measured and compared the rate capability of all electrodes and present the results in Figure 5. The measurement was carried out with an increasing discharge current density at C/20~10 C, and then we decreased it back to C/20. It can be seen that $LiMn_{0.92}Ni_{0.04}Co_{0.04}PO_4$ exhibited a capacity of 89 mA h g^{-1}, which is a much better rate performance than the others at a high current density of 10 C. As for the pure $LiMnPO_4$ samples, they showed poorer behavior, 57 mA h g^{-1} at 10 C. These results might be understood by the proposed mechanism of Mn-sited substituted $LiMnPO_4$ demonstrated by Wang et al. They demonstrated that the Mn-sited substituted $LiMnPO_4$ denoted improved electronic conductivity by changing the electronic structure of $LiMnPO_4$ in virtue of the empty orbits in dopant ions [32]. Similar to this, the electronic conductivity of Co-/Ni-doped $LiMnPO_4$ can be enhanced by changing the electronic structure of $LiMnPO_4$, because there are empty orbits in Co^{2+} ($3d^7$) and Ni^{2+} ($3d^8$), which provide impurity energy levels in the Co-/Ni-doped $LiMnPO_4$. In this way, the kinetics of Co-/Ni-doped $LiMnPO_4$ were substantially developed. Therefore, we concluded that the origins of enhanced kinetics for the Co-/Ni-doped $LiMnPO_4$ were both the proper particle morphology and the changing electronic structure.

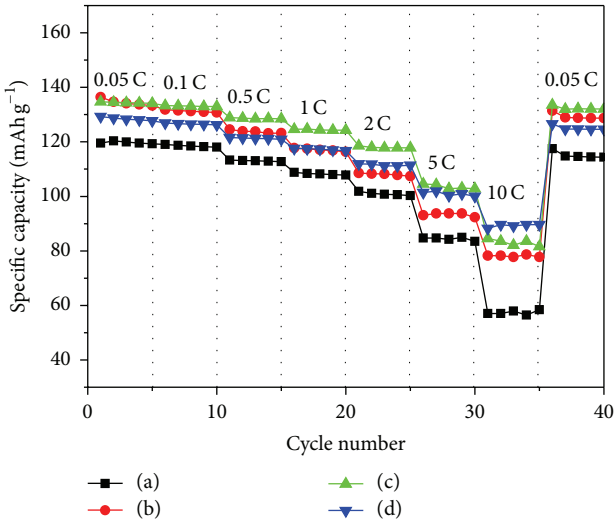

FIGURE 5: Rate capability of (a) pristine, (b) Ni-doped, (c) Co-doped, and (d) Co-/Ni-doped $LiMnPO_4$.

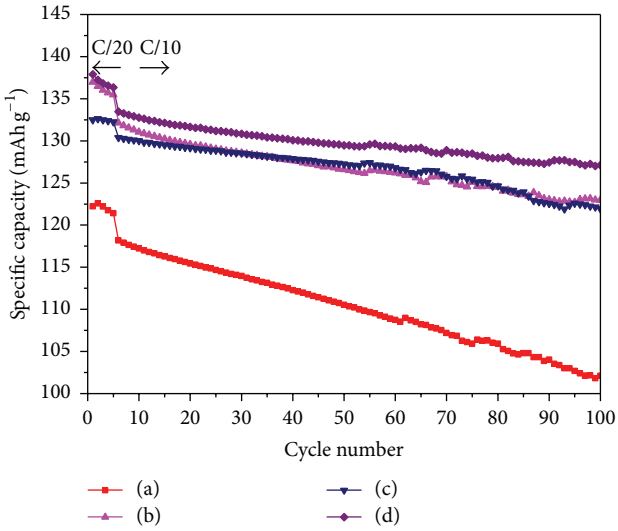

FIGURE 6: Cycling performances of (a) pristine, (b) Ni-doped, (c) Co-doped, and (d) Co-/Ni-doped $LiMnPO_4$ at C/10.

To support these results, the cycling stability of discussed samples under current density at C/10 is shown in Figure 6. The capacity retention of $LiMn_{0.9}Ni_{0.1}PO_4$, $LiMn_{0.9}Co_{0.1}PO_4$, and $LiMn_{0.92}Ni_{0.04}Co_{0.04}PO_4$ after 100 cycles was 90, 92, and 92%, respectively, whereas that of $LiMnPO_4$ was 82%, which is significantly lower than the other samples. The problem of rapid capacity fading is the constantly emerged inactive material caused by the structure destruction during Li^+-ions lithiation and delithiation [33, 34].

In addition, the cycling stability diminishes due to the Jahn-Teller distortion and low ionic conductivity of $LiMnPO_4$. Many researchers have reported that the cation-doped $LiMnPO_4$ exhibits an improvement in cycle life and rate capability. Ni and Gao reported that copper doping on $LiMnPO_4$ resulted in improvement in the discharge capacity and cycle life [35].

4. Conclusions

We developed and synthesized olivine-type $LiMnPO_4$ and cation-doped $Li(Mn, M)PO_4$ ($M = Co^{2+/3+}$, $Ni^{2+/3+}$) electrode materials by a microwave-assisted hydrothermal method and investigated their electrochemical performance. The cation doping on the $LiMnPO_4$ resulted in significant enhancement in the electrode performance with excellent cycle life, higher capacity, and greater rate capability compared with that of pristine $LiMnPO_4$ due to the improved ionic and electronic conductivity. In particular, the $LiMn_{0.92}Co_{0.04}Ni_{0.04}PO_4$ acquired a substantial capacity retention of 92% after 100 cycles, exhibiting a capacity of 134 mA h g^{-1} at 0.05 C and 89 mA h g^{-1} at 10 C, whereas $LiMnPO_4$ had a capacity retention of 82% after 100 cycles with a capacity of 115 mA h g^{-1} at 0.05 C and 57 mA h g^{-1} at 10 C. Our results clearly demonstrated the improvement in performance of $LiMnPO_4$ through the cation doping.

Conflict of Interests

The authors declare that there is no conflict of interests regarding the publication of this paper.

Acknowledgments

This work was supported by the key project of the Korea Research Institute of chemical technology. This research was also supported by Global Frontier Program through the Global Frontier Hybrid Interface Materials (GFHIM) of the National Research Foundation of Korea (NRF) funded by the Ministry of Science, ICT & Future Planning (2013M3A6B1078874).

References

[1] V. Etacheri, R. Marom, R. Elazari, G. Salitra, and D. Aurbach, "Challenges in the development of advanced Li-ion batteries: a review," *Energy & Environmental Science*, vol. 4, no. 9, pp. 3243–3262, 2011.

[2] P. G. Bruce, B. Scrosati, and J.-M. Tarascon, "Nanomaterials for rechargeable lithium batteries," *Angewandte Chemie—International Edition*, vol. 47, no. 16, pp. 2930–2946, 2008.

[3] S. K. Martha, B. Markovsky, J. Grinblat et al., "$LiMnPO_4$ as an advanced cathode material for rechargeable lithium batteries," *Journal of the Electrochemical Society*, vol. 156, no. 7, pp. A541–A552, 2009.

[4] A. K. Padhi, K. S. Nanjundaswamy, and J. B. Goodenough, "Phospho-olivines as positive-electrode materials for rechargeable lithium batteries," *Journal of the Electrochemical Society*, vol. 144, no. 4, pp. 1188–1194, 1997.

[5] T. Nakamura, Y. Miwa, M. Tabuchi, and Y. Yamada, "Structural and surface modifications of $LiFePO_4$ olivine particles and their electrochemical properties," *Journal of the Electrochemical Society*, vol. 153, no. 6, pp. A1108–A1114, 2006.

[6] S.-M. Oh, S.-T. Myung, J. B. Park, B. Scrosati, K. Amine, and Y.-K. Sun, "Double-structured $LiMn_{0.85}Fe_{0.15}PO_4$ coordinated with $LiFePO_4$ for rechargeable lithium batteries," *Angewandte Chemie—International Edition*, vol. 51, no. 8, pp. 1853–1856, 2012.

[7] X.-L. Pan, C.-Y. Xu, D. Hong, H.-T. Fang, and L. Zhen, "Hydrothermal synthesis of well-dispersed $LiMnPO_4$ plates for lithium ion batteries cathode," *Electrochimica Acta*, vol. 87, pp. 303–308, 2013.

[8] G. Yang, H. Ni, H. Liu et al., "The doping effect on the crystal structure and electrochemical properties of $LiMn_xM_{1-x}PO_4$ (M = Mg, V, Fe, Co, Gd)," *Journal of Power Sources*, vol. 196, no. 10, pp. 4747–4755, 2011.

[9] M. K. Devaraju and I. Honma, "Hydrothermal and solvothermal process towards development of $LiMnPO_4$ (M = Fe, Mn) nanomaterials for lithium-ion batteries," *Advanced Energy Materials*, vol. 2, no. 3, pp. 284–297, 2012.

[10] D. Choi, D. Wang, I.-T. Bae et al., "$LiMnPO_4$ nanoplate grown via solid-state reaction in molten hydrocarbon for Li-ion battery cathode," *Nano Letters*, vol. 10, no. 8, pp. 2799–2805, 2010.

[11] N. N. Bramnik and H. Ehrenberg, "Precursor-based synthesis and electrochemical performance of $LiMnPO_4$," *Journal of Alloys and Compounds*, vol. 464, no. 1-2, pp. 259–264, 2008.

[12] M. Pivko, M. Bele, E. Tchernychova, N. Z. Logar, R. Dominko, and M. Gaberscek, "Synthesis of nanometric $LiMnPO_4$ via a two-step technique," *Chemistry of Materials*, vol. 24, no. 6, pp. 1041–1047, 2012.

[13] H.-C. Dinh, S.-I. Mho, Y. Kang, and I.-H. Yeo, "Large discharge capacities at high current rates for carbon-coated $LiMnPO_4$ nanocrystalline cathodes," *Journal of Power Sources*, vol. 244, pp. 189–195, 2013.

[14] S. K. Martha, J. Grinblat, O. Haik et al., "$LiMn_{0.8}Fe_{0.2}PO_4$: an advanced cathode material for rechargeable lithium batteries," *Angewandte Chemie—International Edition*, vol. 48, no. 45, pp. 8559–8563, 2009.

[15] Z. Qin, X. Zhou, Y. Xia, C. Tang, and Z. Liu, "Morphology controlled synthesis and modification of high-performance $LiMnPO_4$ cathode materials for Li-ion batteries," *Journal of Materials Chemistry*, vol. 22, no. 39, pp. 21144–21153, 2012.

[16] J. Hu, J. Xie, X. Zhao et al., "Doping effects on electronic conductivity and electrochemical performance of $LiFePO_4$," *Journal of Materials Science and Technology*, vol. 25, no. 3, pp. 405–409, 2009.

[17] J.-W. Lee, M.-S. Park, B. Anass, J.-H. Park, M.-S. Paik, and S.-G. Doo, "Electrochemical lithiation and delithiation of $LiMnPO_4$: effect of cation substitution," *Electrochimica Acta*, vol. 55, no. 13, pp. 4162–4169, 2010.

[18] J. S. Kim, D.-H. Seo, S.-W. Kim, Y.-U. Park, and K. Kang, "Mn based olivine electrode material with high power and energy," *Chemical Communications*, vol. 46, no. 8, pp. 1305–1307, 2010.

[19] L. Wang, Y. Huang, R. Jiang, and D. Jia, "Preparation and characterization of nano-sized $LiFePO_4$ by low heating solid-state coordination method and microwave heating," *Electrochimica Acta*, vol. 52, no. 24, pp. 6778–6783, 2007.

[20] I. Bilecka and M. Niederberger, "Microwave chemistry for inorganic nanomaterials synthesis," *Nanoscale*, vol. 2, no. 8, pp. 1358–1374, 2010.

[21] N. Li, C. Hu, and M. Cao, "Enhanced microwave absorbing performance of CoNi alloy nanoparticles anchored on a spherical carbon monolith," *Physical Chemistry Chemical Physics*, vol. 15, no. 20, pp. 7685–7689, 2013.

[22] Y. Liu, Y. Zhao, Y. Yu, J. Li, M. Ahmad, and H. Sun, "Hierarchical $CoNiO_2$ structures assembled from mesoporous nanosheets with tunable porosity and their application as lithium-ion battery electrodes," *New Journal of Chemistry*, vol. 38, no. 7, pp. 3084–3091, 2014.

[23] M.-H. Lee, T.-H. Kim, Y. S. Kim, and H.-K. Song, "Precipitation revisited: shape control of $LiFePO_4$ nanoparticles by combinatorial precipitation," *The Journal of Physical Chemistry C*, vol. 115, no. 25, pp. 12255–12259, 2011.

[24] S. Bodoardo, C. Gerbaldi, G. Meligrana, A. Tuel, S. Enzo, and N. Penazzi, "Optimisation of some parameters for the preparation of nanostructured $LifePO_4$/C cathode," *Ionics*, vol. 15, no. 1, pp. 19–26, 2009.

[25] L. Zhang, Q. Qu, L. Zhang, J. Li, and H. Zheng, "Confined synthesis of hierarchical structured $LiMnPO_4$/C granules by a facile surfactant-assisted solid-state method for high-performance lithium-ion batteries," *Journal of Materials Chemistry A*, vol. 2, no. 3, pp. 711–719, 2014.

[26] Q. Lu, G. S. Hutchings, Y. Zhou, H. L. Xin, H. Zheng, and F. Jiao, "Nanostructured flexible Mg-modified $LiMnPO_4$ matrix as high-rate cathode materials for Li-ion batteries," *Journal of Materials Chemistry A*, vol. 2, no. 18, pp. 6368–6373, 2014.

[27] M.-R. Yang and W.-H. Ke, "The doping effect on the electrochemical properties of $LiFe_{0.95}M_{0.05}PO_4$ (M = Mg^{2+}, Ni^{2+}, Al^{3+}, or V^{3+}) as cathode materials for lithium-ion cells," *Journal of the Electrochemical Society*, vol. 155, no. 10, pp. A729–A732, 2008.

[28] D. Jang, K. Palanisamy, Y. Kim, and W. S. Yoon, "Structural and electrochemical properties of doped $liFe_{0.48}Mn_{0.48}Mg_{0.04}PO_4$ as cathode material for lithium ion batteries," *Journal of Electrochemical Science and Technology*, vol. 4, no. 3, pp. 102–107, 2013.

[29] G. Chen, X. Song, and T. J. Richardson, "Electron microscopy study of the $LiFePO_4$ to $FePO_4$ phase transition," *Electrochemical and Solid-State Letters*, vol. 9, no. 6, pp. A295–A298, 2006.

[30] D. Morgan, A. van der Ven, and G. Ceder, "Li conductivity in Li_xMPO_4 (M = Mn, Fe, Co, Ni) olivine materials," *Electrochemical and Solid-State Letters*, vol. 7, no. 2, pp. A30–A32, 2004.

[31] M. S. Islam, D. J. Driscoll, C. A. J. Fisher, and P. R. Slater, "Atomic-scale investigation of defects, dopants, and lithium transport in the $LiFePO_4$ olivine-type battery material," *Chemistry of Materials*, vol. 17, no. 20, pp. 5085–5092, 2005.

[32] D. Wang, C. Ouyang, T. Dŕzen et al., "Improving the electrochemical activity of $LiMnPO_4$ via mn-site substitution," *Journal of the Electrochemical Society*, vol. 157, no. 2, pp. A225–A229, 2010.

[33] X.-G. Gao, G.-R. Hu, Z.-D. Peng, and K. Du, "$LiFePO_4$ cathode power with high energy density synthesized by water quenching treatment," *Electrochimica Acta*, vol. 54, no. 21, pp. 4777–4782, 2009.

[34] J. F. Ni, H. H. Zhou, J. T. Chen, and X. X. Zhang, "$LiFePO_4$ doped with ions prepared by co-precipitation method," *Materials Letters*, vol. 59, no. 18, pp. 2361–2365, 2005.

[35] J. Ni and L. Gao, "Effect of copper doping on $LiMnPO_4$ prepared via hydrothermal route," *Journal of Power Sources*, vol. 196, no. 15, pp. 6498–6501, 2011.